Transport in Porous Media **53:** 39–50, 2003.

Properties of Elastic Waves in a Non-Newtonian (Maxwell) Fluid-Saturated Porous Medium

DAVID TSIKLAURI[1] and IGOR BERESNEV[2]
[1]*Physics Department, University of Warwick, CV4 7AL, Coventry, U.K.*
e-mail: tsikd@astro.warwick.ac.uk
[2]*Department of Geological and Atmospheric Sciences, Iowa State University, 253 Science I, Ames, IA 50011-3212, U.S.A. e-mail: beresnev@iastate.edu*

(Received: 14 January 2002; in final form: 11 June 2002)

Abstract. The present study investigates novelties brought into the classic Biot's theory of propagation of elastic waves in a fluid-saturated porous solid by inclusion of non-Newtonian effects that are important, for example, for hydrocarbons. Based on our previous results (Tsiklauri and Beresnev, 2001), we investigated the propagation of rotational and dilatational elastic waves by calculating their phase velocities and attenuation coefficients as a function of frequency. We found that the replacement of an ordinary Newtonian fluid by a Maxwell fluid in the fluid-saturated porous solid results in: (a) an overall increase of the phase velocities of both the rotational and dilatational waves. With the increase of frequency these quantities tend to a fixed, higher level, as compared to the Newtonian limiting case, which does not change with the decrease of the Deborah number α. (b) The overall decrease of the attenuation coefficients of both the rotational and dilatational waves. With the increase of frequency these quantities tend to a progressively lower level, as compared to the Newtonian limiting case, as α decreases. (c) Appearance of oscillations in all physical quantities in the deeply non-Newtonian regime.

Key words: fluid-saturated porous medium, Biot's theory, non-Newtonian fluids, Maxwell fluid, elastic waves, phase velocities, attenuation coefficients.

1. Introduction

Apart from fundamental interest, there are at least three major reasons for studying the dynamics of fluid in porous media under oscillatory pressure gradient and oscillating pore walls, as well as to investigate propagation of elastic waves in porous media.

First, in petroleum geophysics, regional exploration seismology needs direct methods of discovering oil-filled bodies of rock, and these should be based on models of propagation of elastic waves in porous media with *realistic fluid rheologies* (Carcione and Quiroga-Goode, 1996).

Second, the investigation of the dynamics of fluid in porous media under oscillatory pressure gradient is of prime importance for the recently emerged technology of acoustic stimulation of oil reservoirs (Beresnev and Johnson, 1994; Drake and Beresnev, 1999). It is known that the natural pressure in an oil reservoir generally

yields no more than approximately 10% oil recovery. The residual oil is difficult to produce due to its naturally low mobility, and the enhanced oil recovery operations are used to increase production. It has been experimentally proven that there is a substantial increase in the net fluid flow through porous space if the latter is treated with elastic waves (Beresnev and Johnson, 1994; Drake and Beresnev, 1999).

Third, in environment conservation, treatment of groundwater aquifers contaminated by organic liquids, such as hydrocarbons, by elastic waves proved to be successful for quick and efficient clean-up (Beresnev and Johnson, 1994; Drake and Beresnev, 1999).

A quantitative theory of propagation of elastic waves in a fluid-saturated porous solid was formulated in the classic papers by Biot (1956a, b). One of the major findings of Biot's work was that there is a breakdown in Poisseuille flow above a certain characteristic frequency specific to the fluid-saturated porous material. Biot theoretically studied this phenomenon by considering the flow of a viscous fluid in a tube with longitudinally oscillating walls under an oscillatory pressure gradient. In Biot's theory, the two-phase material is considered a continuum and the microscopic, pore-level effects are ignored. As a reminder, the theory assumes that: (a) the wavelength is large with respect to the dimensions of pores in order to make continuum mechanics applicable; this also implies that scattering dissipation is negligible; (b) the displacements are small, and therefore the macroscopic strain tensor is related to them by the lowest second-order approximation; (c) the liquid phase is continuous, such that the pores are connected, and isolated pores are treated as part of solid matrix; and (d) the permeability is isotropic and the medium is fully saturated.

Biot demonstrated the existence of the two kinds of compressional waves in a fluid-saturated porous medium: the fast wave for which the solid and fluid displacements are in phase, and the slow wave for which the displacements are out of phase. At low frequencies, the medium does not support the slow wave as it becomes diffusive. On the other hand, at high frequencies, tangential slip takes place, inertial effects dominate, and the slow wave becomes activated.

Biot's theory can be used to describe interaction of fluid-saturated solid with the sound for a classic Newtonian fluid; however, oil and other hydrocarbons often exhibit significant non-Newtonian behavior. In Paper I (Tsiklauri and Beresnev, 2001), we have incorporated non-Newtonian effects into the classic theory of Biot (1956a, b). Using the recent results of del Rio *et al.* (1998), who presented a study of enhancement in the dynamic response of a viscoelastic (Maxwell) fluid flowing through a stationary (non-oscillating) tube under the effect of an oscillatory pressure gradient, we have combined their theory with the effect of the acoustic oscillations of the walls of the tube introduced by Biot (1956a, b), thus providing a complete description of the interaction of Maxwell fluid, filling the pores, with acoustic waves. We have generalized the expression for the function $F(\kappa)$, which measures the deviation from Poisseuille flow friction as a function of frequency parameter κ (Tsiklauri and Beresnev, 2001). As a next step, in the present work we

investigate the propagation of rotational and dilatational elastic waves through the porous medium filled with Maxwell fluid, by calculating their phase velocities and attenuation coefficients as a function of frequency.

This paper is organized as follows: we formulate theoretical basis for our numerical calculations in Section 2. In Sections 3 and 4, we study numerically properties of the rotational and dilatational elastic waves, respectively, and, finally, in Section 5 we close with a discussion of our main results.

2. Theory

The theory of propagation of elastic waves in a fluid-saturated porous solid was formulated by Biot (1956a, b). He demonstrated that the general equations which govern propagation of rotational and dilatational high-frequency waves in a fluid-saturated porous medium are the same as in the low-frequency range, provided the viscosity is replaced by its effective value as a function of frequency. In practice, it means replacing the resistance coefficient b by $bF(\kappa)$.

The equations describing dynamics of the rotational waves are (Biot, 1956a, b)

$$\frac{\partial^2}{\partial t^2}(\rho_{11}\vec{\omega} + \rho_{12}\vec{\Omega}) + bF(\kappa)\frac{\partial}{\partial t}(\vec{\omega} - \vec{\Omega}) = N\nabla^2\vec{\omega}, \tag{1}$$

$$\frac{\partial^2}{\partial t^2}(\rho_{12}\vec{\omega} + \rho_{22}\vec{\Omega}) - bF(\kappa)\frac{\partial}{\partial t}(\vec{\omega} - \vec{\Omega}) = 0, \tag{2}$$

where, ρ_{11}, ρ_{12} and ρ_{22} are mass density parameters for the solid and fluid and their inertia coupling; $\vec{\omega} = \text{curl } \vec{u}$ and $\vec{\Omega} = \text{curl } \vec{U}$ describe rotations of solid and fluid with $\vec{u}$ and $\vec{U}$ being their displacement vectors, while the rigidity of the solid is represented by the modulus N. Substitution of a plane rotational wave of the form

$$\omega = C_1 e^{i(lx+\chi t)}, \qquad \Omega = C_2 e^{i(lx+\chi t)}, \tag{3}$$

into Equations (1) and (2) allows us to obtain a characteristic equation

$$\frac{Nl^2}{\rho\chi^2} = E_r - iE_i, \tag{4}$$

where l is wavenumber, $\chi = 2\pi f$ is wave cyclic frequency, $\rho = \rho_{11} + 2\rho_{12} + \rho_{22}$ is the mass density of the bulk material.

The real and imaginary parts of Equation (4) can be written as

$$E_r = \frac{(\gamma_{11}\gamma_{22} - \gamma_{12}^2)(\gamma_{22} + \epsilon_2) + \gamma_{22}\epsilon_2 + \epsilon_1^2 + \epsilon_2^2}{(\gamma_{22} + \epsilon_2)^2 + \epsilon_1^2}, \tag{5}$$

and

$$E_i = \frac{\epsilon_1(\gamma_{12} + \gamma_{22})^2}{(\gamma_{22} + \epsilon_2)^2 + \epsilon_1^2}, \tag{6}$$

where $\gamma_{ij} = \rho_{ij}/\rho$, $\epsilon_1 = (\gamma_{12} + \gamma_{22})(f_c/f)\, Re[F(\kappa)] = (\gamma_{12} + \gamma_{22})(f_c/f)\, Re[F(\delta\sqrt{f/f_c})]$, $\epsilon_2 = (\gamma_{12} + \gamma_{22})(f_c/f)\, Im[F(\kappa)] = (\gamma_{12} + \gamma_{22})(f_c/f)\, Im[F(\delta\sqrt{f/f_c})]$. The function $F(\kappa)$ was written here more conveniently as a function of frequency f, that is, $F(\kappa) = F(\delta\sqrt{f/f_c})$ (Biot, 1956a, b), where δ is a factor dependent on pore geometry. For the hollow cylinder-like pores, $\delta = \sqrt{8}$ (Biot, 1956a, b) and we use this value throughout the paper. f_c is the critical frequency above which the Poisseuille flow breaks down, and it equals $b/(2\pi\rho_2) = b/(2\pi\rho(\gamma_{12} + \gamma_{22}))$.

To obtain phase velocity and attenuation coefficient of the rotational waves, we put $l = Re[l] + iIm[l]$. Thus, the phase velocity is then $v_r = \chi/|Re[l]|$. Introducing a reference velocity as $V_r = \sqrt{N/\rho}$, we obtain the dimensionless phase velocity as

$$\frac{v_r}{V_r} = \frac{\sqrt{2}}{\left[\sqrt{E_i^2 + E_r^2} + E_r\right]^{1/2}}. \tag{7}$$

To obtain the attenuation coefficient of the rotational waves, we introduce a reference length, L_r, defined as $L_r = V_r/(2\pi f_c)$. The length x_a represents the distance over which the rotational wave amplitude is attenuated by a factor of $1/e$. Therefore, we can construct the dimensionless attenuation coefficient as L_r/x_a,

$$\frac{L_r}{x_a} = \frac{f}{f_c}\frac{\left[\sqrt{E_i^2 + E_r^2} - E_r\right]^{1/2}}{\sqrt{2}}. \tag{8}$$

The equations describing dynamics of the dilatational waves are (Biot, 1956a, b)

$$\nabla^2(Pe + Q\epsilon) = \frac{\partial^2}{\partial t^2}(\rho_{11}e + \rho_{12}\epsilon) + bF(\kappa)\frac{\partial}{\partial t}(e - \epsilon), \tag{9}$$

$$\nabla^2(Qe + R\epsilon) = \frac{\partial^2}{\partial t^2}(\rho_{12}e + \rho_{22}\epsilon) - bF(\kappa)\frac{\partial}{\partial t}(e - \epsilon), \tag{10}$$

where, P, Q and R are the elastic coefficients, $e = \text{div}\ \vec{u}$ and $\epsilon = \text{div}\ \vec{U}$ are the divergence of solid and fluid displacements. Again, substitution of a plane dilatational wave of the form

$$e = C_1 e^{i(lx+\chi t)}, \qquad \epsilon = C_2 e^{i(lx+\chi t)}, \tag{11}$$

into Equations (9) and (10) allows us to obtain a characteristic equation

$$(z - z_1)(z - z_2) + iM(z - 1) = 0, \tag{12}$$

where $z = l^2V_c^2/\chi^2$, $V_c^2 = (P+R+2Q)/\rho$ represents the velocity of a dilatational wave when the relative motion between fluid and solid is absent, $z_{1,2} = V_c^2/V_{1,2}^2$

with $V_{1,2}$ being the velocities of the purely elastic waves with subscripts 1, 2 referring to the two roots of Equation (12), and finally $M = (\epsilon_1 + i\epsilon_2)/(\sigma_{11}\sigma_{22} - \sigma_{12}^2)$ with $\sigma_{11} = P/(P+R+2Q)$, $\sigma_{22} = R/(P+R+2Q)$ and $\sigma_{12} = Q/(P+R+2Q)$.

Equation (12) has two complex roots z_I and z_{II}. Phase velocities of the two kinds of dilatational waves can be defined as

$$\frac{v_I}{V_c} = \frac{1}{Re[\sqrt{z_I}]}, \qquad \frac{v_{II}}{V_c} = \frac{1}{Re[\sqrt{z_{II}}]}, \tag{13}$$

while the corresponding attenuation coefficients can be also introduced as

$$\frac{L_c}{x_I} = Im[\sqrt{z_I}]\frac{f}{f_c}, \qquad \frac{L_c}{x_{II}} = Im[\sqrt{z_{II}}]\frac{f}{f_c}. \tag{14}$$

In Paper I, we generalized Biot's expression for $F(\kappa)$ to the case of a non-Newtonian (Maxwell) fluid, which reads

$$F(\kappa) = -\frac{1}{4}\frac{\kappa\sqrt{i+\kappa^2/\alpha}\left[J_1(\kappa\sqrt{i+\kappa^2/\alpha})/J_0(\kappa\sqrt{i+\kappa^2/\alpha})\right]}{(1-i\kappa^2/\alpha)} \times \times \left[1 - \frac{2J_1(\kappa\sqrt{i+\kappa^2/\alpha})}{\kappa\sqrt{i+\kappa^2/\alpha}\,J_0(\kappa\sqrt{i+\kappa^2/\alpha})}\right]^{-1}. \tag{15}$$

Here, $\kappa = a\sqrt{\omega/\nu}$ is the frequency parameter, a is the radius of the pore, $\nu = \eta/\rho$ is the ratio of the viscosity coefficient to the fluid mass density, J_0 and J_1 are the Bessel functions, and, finally, α denotes the Deborah number del Rio *et al.* (1998), which is defined as the ratio of the characteristic time of viscous effects $t_v = a^2/\nu$ to the relaxation time t_m, that is, $\alpha = t_v/t_m = a^2/(\nu t_m)$.

Equation (15) was derived by solving the equations of incompressible hydrodynamics, namely, the continuity equation, linearized momentum equation, and rheological equation of a Maxwell fluid, in the frequency domain for a cylindrical tube whose walls oscillate harmonically in time. By calculating the ratio of the total friction force exerted on the tube wall to the average velocity of a Maxwell fluid, and noting that $F(\kappa)$ is proportional to this ratio, we generalized the classical result obtained by Biot (see details in Paper I).

As noted in del Rio *et al.* (1998), the value of the parameter α determines in which regime the system resides. Beyond a certain critical value ($\alpha_c = 11.64$), the system is dissipative, and viscous effects dominate. On the other hand, for small α ($\alpha < \alpha_c$), the system exhibits viscoelastic behavior which we call the non-Newtonian regime. Note that the Newtonian flow regime can be easily recovered from Equation (15) by putting $\alpha \to \infty$.

To investigate the novelties brought into the classic Biot's theory of propagation of elastic waves in porous medium (Biot, 1956a, b) by the inclusion of non-Newtonian effects, we have studied the full parameter space of the problem. We have calculated the normalized phase velocities and attenuation coefficients for

both rotational and dilatational waves using our general expression for $F(\kappa)$ given by Equation (15).

3. Numerical Results for Propagation of Rotational Waves

In all our numerical calculations, we have used polynomial expansions of J_0 and J_1 with absolute error not exceeding $10^{-6}\%$. Thus, our calculation results are accurate to this order. Also, in order to catch a true oscillatory structure of our solutions (see below), number of data points in all our plots is 10 000, as opposed to Paper I where only 100 points per curve were taken.

In all forthcoming results, we calculate phase velocities and attenuation coefficients for the case 1 from Table I taken from (Biot, 1956b), which is $\sigma_{11} = 0.610$, $\sigma_{22} = 0.305$, $\sigma_{12} = 0.043$, $\gamma_{11} = 0.500$, $\gamma_{22} = 0.500$, $\gamma_{12} = 0$, $z_1 = 0.812$, and $z_2 = 1.674$.

We calculated normalized phase velocity of the plane rotational waves, v_r/V_r, and the attenuation coefficient L_r/x_a using our more general expression for $F(\kappa)$ (Maxwell fluid filling the pores) given by Equation (15).

In Figure 1 we plot phase velocity v_r/V_r as a function of frequency for the three cases: the thick curve corresponds to $\alpha \to \infty$ (Newtonian limit), the dashed curve corresponds to a slightly sub-critical value of $\alpha = 10$ (recall that $\alpha_c = 11.64$) and thin solid curve corresponds to the case of $\alpha = 1$. Note that the $\alpha \to \infty$ case perfectly reproduces the curve 1 in Figure 5 from (Biot, 1956b). For $\alpha = 10$ we notice a deviation from the classic Newtonian behavior in the form of overall increase of phase velocity and appearance of small oscillations on the curve, which means that we have entered the non-Newtonian regime. Note that when $\alpha = 1$ the phase velocity settles at somewhat higher value and this onset happens already

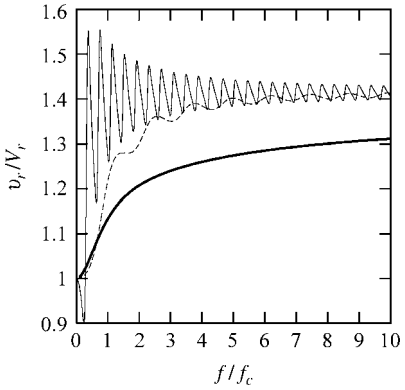

Figure 1. Behavior of dimensionless, normalized phase velocity of the rotational wave, v_r/V_r, as a function of frequency. The thick solid curve corresponds to the Newtonian limit when $\alpha \to \infty$, while dashed and thin solid curves represent the non-Newtonian cases $\alpha = 10$ and $\alpha = 1$, respectively.

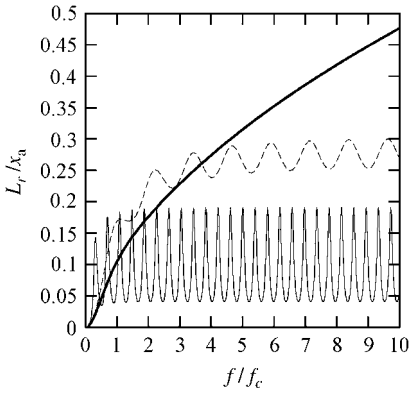

Figure 2. Behavior of dimensionless, normalized attenuation coefficient of the rotational wave, L_r/x_a, as a function of frequency. The thick solid curve corresponds to the Newtonian limit when $\alpha \to \infty$, while dashed and thin solid curves represent the non-Newtonian cases $\alpha = 10$ and $\alpha = 1$, respectively.

for smaller frequencies than in the case of Newtonian fluid. Also, a much more pronounced oscillatory structure of the solution can be observed.

Figure 2 shows the attenuation coefficient L_r/x_a of the rotational wave as a function of frequency for the three values of α: the thick curve corresponds to $\alpha \to \infty$ (Newtonian limit), the dashed curve corresponds to a slightly sub-critical value of $\alpha = 10$ and thin solid curve corresponds to the case of $\alpha = 1$. Note that $\alpha \to \infty$ case coincides with curve 1 in Figure 6 from (Biot, 1956b). For $\alpha = 10$, there is a noticeable deviation from the classic Newtonian behavior in the form of overall decrease of the attenuation coefficient and appearance of small oscillations on the curve indicating that the wave has entered the non-Newtonian regime. For $\alpha = 1$, the attenuation coefficient settles at a somewhat lower value, and this happens already for smaller frequencies than in the case of Newtonian fluid. Also, a much more pronounced oscillatory structure of the solution can be noticed.

4. Numerical Results for Propagation of Dilatational Waves

We calculated normalized phase velocities of the plane dilatational waves, v_I/V_c and v_{II}/V_c, and the attenuation coefficients L_c/x_I and L_c/x_{II} using our more general expression for $F(\kappa)$ (Maxwell fluid filling the pores) given by Equation (15).

In Figure 3 we plot phase velocity v_I/V_c as a function of frequency for the case of $\alpha \to \infty$, in order to recover the Newtonian limit obtained by Biot. Note that this case reproduces curve 1 in Figure 11 from Biot (1956b).

Figure 4 shows phase velocity v_I/V_c as a function of frequency for the case of $\alpha = 1$, corresponding to the deeply non-Newtonian regime. We notice again the appearance of an oscillatory structure of the solution. Also, phase velocity v_I/V_c

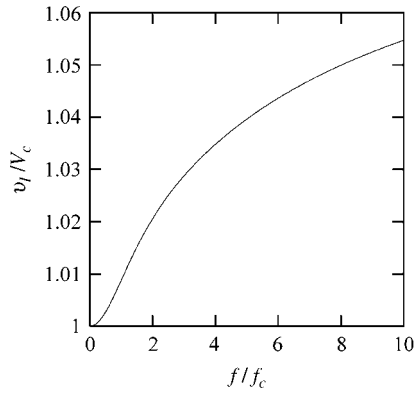

Figure 3. Behavior of dimensionless, normalized phase velocity of the dilatational wave, v_I/V_c, as a function of frequency. Here the Newtonian limiting case, when $\alpha \to \infty$, is plotted.

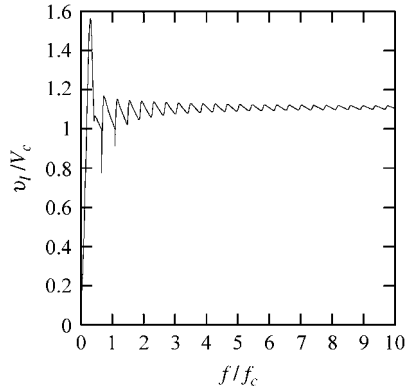

Figure 4. Same as in Figure 3 but for $\alpha = 1$.

settles at a somewhat higher value than in the Newtonian case, and this happens already for smaller frequencies.

In Figure 5 we plot phase velocity v_{II}/V_c as a function of frequency for the cases of $\alpha \to \infty$ and $\alpha = 1$. Note that the case of $\alpha \to \infty$ (thick solid line) perfectly reproduces the Newtonian limit obtained by Biot curve 1 in Figure 12 from Biot (1956b). For $\alpha = 1$, again we notice an oscillatory structure of the solution. Besides, we observe that the phase velocity v_{II}/V_c settles again at a somewhat higher value than in the Newtonian case.

In Figure 6 we plot the attenuation coefficient L_c/x_I as a function of frequency for the three cases: the thick curve corresponds to $\alpha \to \infty$ (Newtonian limit), the dashed curve corresponds to a slightly sub-critical value of $\alpha = 10$ and thin solid curve corresponds to the case of $\alpha = 1$. The $\alpha \to \infty$ case reproduces curve 1 in Figure 13 from Biot (1956b). For $\alpha = 10$, we notice deviation from the classic Newtonian behavior in the form of the overall increase of the attenuation coefficient and appearance of small oscillations on the curve, which indicates that the wave has

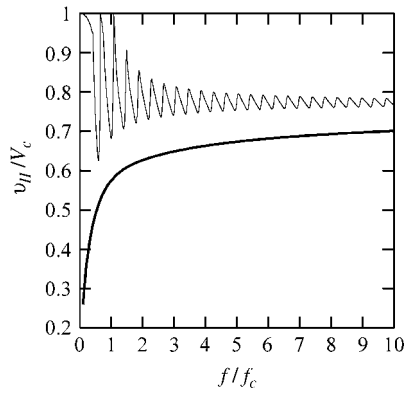

Figure 5. Behavior of dimensionless, normalized phase velocity of the dilatational wave, v_{II}/V_c, as a function of frequency. Here the Newtonian limiting case, when $\alpha \to \infty$, is plotted with thick curve, while the thin one corresponds to the non-Newtonian case of $\alpha = 1$.

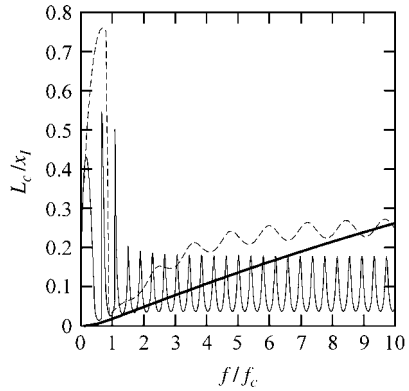

Figure 6. Behavior of dimensionless, normalized attenuation coefficient of the dilatational wave, L_c/x_I, as a function of frequency. The thick solid curve corresponds to the Newtonian limit when $\alpha \to \infty$, while dashed and thin solid curves represent the non-Newtonian cases $\alpha = 10$ and $\alpha = 1$, respectively.

entered the non-Newtonian regime. The large spike at low frequencies is also due to non-Newtonian effects. For the case of $\alpha = 1$ the attenuation coefficient settles at somewhat lower values, and this happens already for smaller frequencies than in the case of a Newtonian fluid. Also, a much more pronounced oscillatory structure of the solution can be noticed.

In Figure 7 we plot the attenuation coefficient L_c/x_{II} as a function of frequency for the three cases: the thick curve corresponds to $\alpha \to \infty$ (Newtonian limit), the dashed curve corresponds to $\alpha = 10$ and thin solid curve corresponds to the case of $\alpha = 1$. Note that the $\alpha \to \infty$ case perfectly matches curve 1 in Figure 14 from Biot (1956b). For $\alpha = 10$, we notice a deviation from the classic Newtonian behavior in the form of the overall decrease in the attenuation coefficient and appearance of small oscillations on the curve. The jump at $f/f_c = 1$

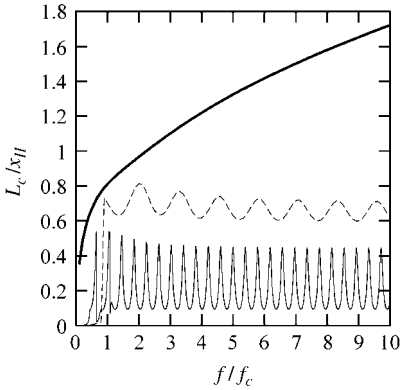

Figure 7. Behavior of dimensionless, normalized attenuation coefficient of the dilatational wave, L_c/x_{II}, as a function of frequency. The thick solid curve corresponds to the Newtonian limit when $\alpha \to \infty$, while dashed and thin solid curves represent the non-Newtonian cases $\alpha = 10$ and $\alpha = 1$, respectively.

(dashed curve) should be attributed to the non-Newtonian effects. For the case of $\alpha = 1$ the attenuation coefficient settles again at somewhat lower value and this happens already for smaller frequencies than in the case of the Newtonian fluid. Also, a much more pronounced oscillatory structure of the solution can be noticed again.

5. Discussion

In this paper, we have studied the non-Newtonian effects in the propagation of elastic waves in porous media by calculating phase velocities and attenuation coefficients of the rotational and dilatational waves as a function of frequency. Originally, Biot (1956a, b) performed similar analysis for a Newtonian fluid-saturated porous medium. Using our recent results (Paper I), and motivated by a current need in models of propagation of elastic waves in porous media with *realistic fluid rheologies*, we have generalized the work of Biot to the case of a non-Newtonian (Maxwell) fluid-saturated porous medium.

In short, we found that replacement of an ordinary Newtonian fluid by a Maxwell fluid in the fluid-saturated porous medium results in

— an overall increase of the phase velocities of both the rotational and dilatational waves. With the increase of frequency these quantities tend to a fixed, higher level, as compared to the Newtonian limiting case, which does not change with the decrease of the Deborah number α.
— the overall decrease of the attenuation coefficients of both the rotational and dilatational waves. With the increase of frequency these quantities tend to a progressively lower level, as compared to the Newtonian limiting case, as α decreases.

— appearance of oscillations in all physical quantities in the deeply non-Newtonian regime when $\alpha \ll \alpha_c = 11.64$.

The investigation of properties of elastic waves is important for a number of applications. The knowledge of phase velocities and attenuation coefficients of elastic waves in a realistic [such as saturated with Maxwell fluid] porous medium is necessary, for example, to guide oilfield exploration applications, acoustic stimulation of oil-producing fields (to increase the amount of recovered residual oil), and the acoustic clean-up of contaminated aquifers (Beresnev and Johnson, 1994; Drake and Beresnev, 1999).

The idea of the paper was to use the function, $F(\kappa)$, that measures the deviation from Poisseuille flow friction, extended to Maxwell fluids, and to substitute it into Biot's equations of poroelasticity without changing the latter. However, Biot's equations have been derived under a number of assumptions. One of these assumptions is that deviatoric (shear) components of the macroscopic stress in the fluid are negligible Pride *et al.* (1992). Pride *et al.* (1992) have shown that this assumption is justified when $\eta\omega \ll G$, where η is the dynamic viscosity of the fluid, ω is frequency, and G is frame shear modulus. Simple analysis shows that for typical Newtonian fluids such as water, this condition is violated only at frequencies $\omega > 10^9$ 1/s, or $f = \omega/(2\pi) > 10^8$ Hz. Thus, for all frequencies below 1 MHz Biot's assumption is justified. However, when we introduce the Maxwell fluid, the situation changes in that we introduce the real (in addition to imaginary) shear stresses. In short, for any rheology (including Maxwellian) Biot's theory is valid only if macroscopic shear stresses are negligible. To prove that, we note from the rheological equation for a Maxwell fluid

$$t_m \frac{\partial \tilde{\tau}}{\partial t} = -\eta \nabla \vec{v} - \tilde{\tau},$$

where $\tilde{\tau}$ represents the viscous stress tensor, that in the frequency domain we can effectively obtain

$$\tilde{\tau} = \frac{-\eta \nabla \vec{v}}{(1 + i t_m \omega)}.$$

This means that we can roughly replace η in all our estimates with $\eta'/(1 + i t_m \omega)$. There are two limiting cases. When $\omega \ll 1/t_m$, then the fluid is effectively Newtonian and Biot's theory is valid. When $\omega \gg 1/t_m$, that is, when the fluid is essentially non-Newtonian, we effectively have $\eta' = \eta/(i t_m \omega)$, which in this case is smaller than η in absolute value. Thus, when substituted into the shear stress, S, it produces $S = i\eta'\omega = \eta/t_m$, which is smaller than $\eta\omega$. Therefore, we conclude that inequality $\eta'\omega \ll G$ still holds for the Maxwellian fluid, that is, Biot's equations are valid for Maxwell rheology.

This study, similar to the results of Paper I, has clearly shown the transition from dissipative to non-Newtonian regime in which sharp oscillations of all physical

quantities are found. We would like to comment on these unexpected strong oscillations that were demonstrated by our numerical analysis. The results are based on Equation (15), which has been derived for a circular cylindrical geometry. This is the same geometry that was used in the classic works of Biot and others. For Newtonian fluids the use of such an idealized geometry for porous materials was backed by an analysis that showed that the results are not very sensitive to the particular geometry (see, e.g. Johnson *et al.*, 1987). Of course, the magnitude of these oscillations depends on fluid parameters and permeability, and may not be as high for many fluids. However, even if parameters are such that oscillations are large, it is unclear at this stage whether this oscillatory behavior will hold for more realistic geometry, that is, when curved pore walls (tortuosity) are considered. There is a possibility that with tortuosity effects included the obtained oscillations will be smeared. However, our goal was to constrain ourselves with simple cylindrical geometry, and a separate study is needed to analyze the tortuosity effects on our results.

Acknowledgements

This work was supported by the Iowa State University Center for Advanced Technology Development and ETREMA Products, Inc.

References

Beresnev, I. A. and Johnson, P. A.: 1994, Elastic-wave stimulation of oil production: A review of methods and results, *Geophys.* **59**, 1000–1017.

Biot, M. A.: 1956a, Theory of propagation of elastic waves in a fluid-saturated porous solid. I. low-frequency range, *J. Acoust. Soc. Am.* **28**, 168–178.

Biot, M. A.: 1956b, Theory of propagation of elastic waves in a fluid-saturated porous solid. II. higher-frequency range, *J. Acoust. Soc. Am.* **28**, 179–191.

Carcione, J. M. and Quiroga-Goode, G.: 1996, Full frequency-range transient solution for compressional waves in a fluid-saturated viscoacoustic porous medium, *Geophys. prospecting* **44**, 99–129.

del Rio, J. A., de Haro, M. L. and Whitaker, S.: 1998, Enhancement in the dynamic response of a viscoelastic fluid flowing in a tube, *Phys. Rev. E* **E58**, 6323–6327.

Drake, T. and Beresnev, I.: 1999, Acoustic tool enhances oil production, *The American Oil & Gas Reporter*, September issue, pp. 101–104.

Johnson, D. L., Koplik, J. and Dashen, R.: 1987, Theory of dynamic permeability and tortousity in a fluid-saturated porous media, *J. Fluid. Mech.* **176**, 379–402.

Pride, S. R., Gangi, A. F. and Morgan, F. D.: 1992, Deriving the equations of motion for porous isotropic media, *J. Acoust. Soc. Am.* **92**, 3278–3290.

Tsiklauri, D. and Beresnev, I.: 2001, Enhancement in the dynamic response of a viscoelastic fluid flowing through a longitudinally vibrating tube, *Phys. Rev. E* **63**, 046304-1-4 (2001), Paper I.